ЖЭТФ, 2023, том 163, вып. 6, стр. 779–785

IONIZATION TRANSITION RATES IN THE INTERMEDIATE REGIME OF THE KELDYSH PARAMETER FOR A (0,1)*LG SPIRAL AMPLITUDE MODULATED LASER FIELD

T. B. Miladinović [a*], ***S. Simić*** [b], ***N. Danilović*** [b]

[a] *Institute for Information Technologies, University of Kragujevac 34000 Kragujevac, Serbia*

[b] *Faculty of Science, University of Kragujevac 34000 Kragujevac, Serbia*

Received January 01, 2023,
revised version January 01, 2023,
Accepted for publication January 25, 2023

DOI: 10.31857/S0044451023060020
EDN: DDLKRB

One of the most probable processes occurring during the interaction of matter with strong laser fields is ionization and a detailed understanding of this process is important to control the dynamics of the newly formed quantum-mechanical systems [1, 2]. The ionization process considers the weakest bound electron which can be freed and moved into a continuum when the laser provides enough energy by adjusting its frequency and intensity [3–6]. Several theories have been developed that provide physical insight into multiphoton and tunnel ionization processes [7–9]. Keldysh [7] showed that multiphoton and tunnel ionization is two boundary cases of the same universal ionization process, determined by three parameters: laser frequency ω, the value of the electric field F and ionization potential I_p. The separation line between these two ionization mechanisms can be defined using the so-called adiabatic parameter, also known as the Keldysh parameter $\gamma = \omega\sqrt{2m_eI_p}/(eF)$. For the weak laser fields, the Keldysh parameter has a large value, $\gamma \gg 1$ and then the multiphoton ionization (MPI) becomes possible, for the strong fields, $\gamma \ll 1$ and consequently corresponds to the tunneling ionization (TI) process. Despite these, it has been noticed that these boundaries did not so strict [10–13], and often were interpreted as $\gamma > 1$ and $\gamma < 1$ [14]. For $\gamma > 1$, tunnel ionization is not impossible, but it is only less probable. It can be considered that with increasing this parameter, ionization can occur through both mechanisms in such a way that the dominant mechanism is transited from TI to MPI. Since the value of the gamma parameter is determined by a set of laser parameters, and by careful selection of those parameters, the photon energy can be in the X-ray region, and then the Keldysh parameter reaches the value of $\gamma \approx 30-100$ [15,16]. In a study that $\gamma \gg 1$ can also be performed by adjusting the laser pulse duration, Topcu and Robicheaux investigated the ionization rate for the value of $\gamma \leq 60$ [17].

In the study of the multiphoton and the tunnel ionization, besides the field strength and pulse duration, the type of polarization of laser light is also important, and numerous theoretical and experimental papers dealt with the influence of the linear, circular and elliptical polarization of laser pulse on these processes [18–20]. Meanwhile, in recent years, greater attention is directed toward radially polarized light, so numerous applications in optical trapping [21], sharp focusing [22], optical lithography [23] and particle acceleration [24, 25] were found. Radially polarized beams have a Laguerre Gaussian (LG) ring intensity distribution with a polarization singularity at the centre and can be created by direct emission from a suitable laser or by manipulating a linearly polarized, lowest-order Gaussian beam. Depending on the required characteristics of the beam, the radial LG beam can be efficiently converted into a fundamental Gaussian beam and vice versa [26, 27]. By implementing and combining a Spatial Light Modulator (SLM) and interferometric technique in the laser system, complex surface patterning of LG beams can generate and create the logarithmic spiral [28].

* E-mail: tanja.miladinovic@uni.kg.ac.rs

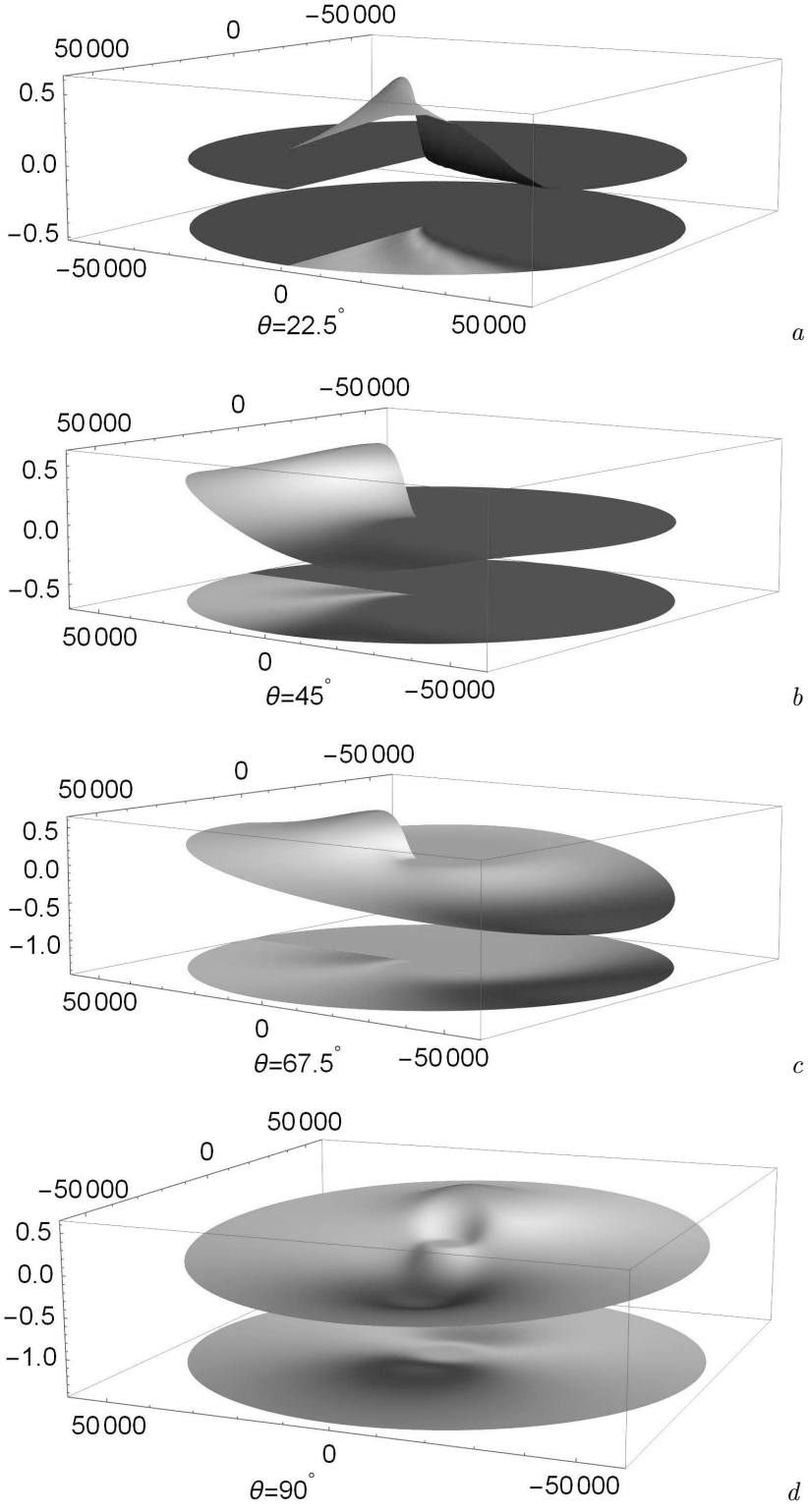

Fig. 1. Electric field distribution $F^{sp}(r,\phi)$ obtained for different angle θ: $\theta = 22.5^\circ$ (a), 45° (b), 67.5° (c), 90° (d)

In this paper, direct ionization of valence electrons is considered when electrons leave an atom and enter directly into the continuum. As the target, the potassium atom is chosen for the reason that ADK formalism is fully compatible with hydrogen-like atoms and the argon atom, a widely used rare-gas atom, which has ionization energy similar to a hydrogen atom. Transition ionization rates of the TI and MPI processes, as well as the total transition rate in the case when ionization occurs due to the combination of these two processes (intermediate regime), were calculated. The results are analyzed and present that an intermediate regime appears at different values of the Keldysh parameter γ, with significant differences (several orders of magnitude) of the transition rates. The calculations were performed for the linearly polarized $(0,1)$*LG laser beam with spiral amplitude modulation in a quite wide range of intensities. The Stark effect and the ponderomotive potential and their effect on the transition rate in the case of this particular laser beam profile are also included in the study. Throughout this paper, all quantities that describe the target and laser field are given in atomic units $\mid e \mid = m_e = \hbar = 1$.

The parameter γ is defined in such a way that TI and MPI processes are specified as two boundary cases corresponding $\gamma \ll 1$ and $\gamma \gg 1$, respectively, and most experiments are performed within these frames [30, 31]. Therefore, it is interesting to study the ionization process in the intermediate regime where both TI and MPI contribute. In this regime, it is hard to explicitly determine which of the ionization mechanisms has a dominant role, only it is expected that $\gamma > 1$. In this particular case it is necessary to use the total transition rate equation $w_{tot}(F,\omega)$ which can be represented as the sum of two Gaussian functions, $f_{tot} = a_{TI,MPI}\exp(-(x - b_{TI,MPI})^2/c^2_{TI,MPI})$. This type of simulation is justified because each of the transition rates, both TI and MPI, calculated individually had a Gaussian shape. This total function has six variables: $a_{TI,MPI}$ the heights of the Gaussian functions, $b_{TI,MPI}$ the positions of maximum values, $c_{TI,MPI}$ widths of two Gaussian functions.

The constant strong external field produces a Stark shift of atomic levels, change effectively the electron ionization potential I_p. Shifting of energy levels deepens the potential barrier and makes it more difficult for atoms to ionize. The energy of the displacement can be calculated as $\delta E = -\alpha F^2/4$ [32,33], where α is the static polarizability of the atom [34]. A significant modification of the ionization potential occurs when the average energy of a free electron oscillating in the electric field, $U_p = F^2/(4\omega^2)$ [35] is accounted. U_p is intensity-dependent ponderomotive energy and has a much higher value than the ionization potential. Including this value in the calculation affects the probability and rate of the ionization process. The effective ionization potential becomes $I_p^{eff} = I_p + \delta E + U_p$. [36, 37].

In this paper, the photoionization process in $(0,1)$*LG beams also known as "vortex" or "doughnut" beams which are circularly symmetric and directly related to the quantized orbital angular momentum (OAM) of photons [38, 39] and electrons [40], is considered. The amplitude of the laser field strength F is constant, but adding a second term to the equation leads to a light field with spatially non-uniform amplitude [41], then the $(0,1)$*LG spiral amplitude modulated laser field distribution [28] is $F^{sp}(r,\phi) = F\sqrt{\rho}e^{-\rho/2}e^{\pm i\phi}$, where r and ϕ are the cylindrical coordinates, sign $\pm$ defines beam helicity and $\rho = 2r^2/R^2$, R is the spot size of the Gaussian beam. $r(\phi) = ae^{k\phi}$ is a polar equation that gives a curve called the logarithmic spiral [42, 43]. k, a are parameters, $k = \mathrm{ctg}\theta$ determines the spiral winding, where $a = 0.57$ (with r in μm). It should be emphasized that the polar equation includes azimuthal ($\theta = 90°$) and radial ($\theta = 0°$) polarization particular cases.

In any beam of light, the energy flux is carried by a Pointing vector. The Pointing vector can be calculated as the vector product of the electric and magnetic fields and always is parallel to the wavevector and perpendicular to the wavefront of the beam [44]. In its most common form, the wavefront of laser light is approximately planar, and the wavevector is directed along the beam axis in the direction of propagation, while the Laguerre-Gaussian beams have intertwined helical wavefronts [45].

In the range of the used intensities, a strong laser field can be treated as a pure electric field, a magnetic field component does not have to be included. Therefore, electric field distribution for $(0,1)$*LG with spiral amplitude modulation, when the spiral geometry of the beam determines with different values of angle θ, is presented in Fig. 1. It can be seen that the beam has field distribution in the form of a lobe depending on the rotation angle. The obtained results emphasize the complexity of electric fields and the possible impact on ionization processes inducted by a $(0,1)$*LG laser field with spiral amplitude modulation. Taking into account that the ionization of the atoms in an alternating field depends on field strength and that the amplitude of the electric component has the form $F^{sp}(r,\phi)$, transformed formulas $I_p^{sp,eff}, w_{TI}^{sp}(F^{sp},\omega,r,\phi)$, $w_{MPI}^{sp}(F,\omega,r,\phi)$ can

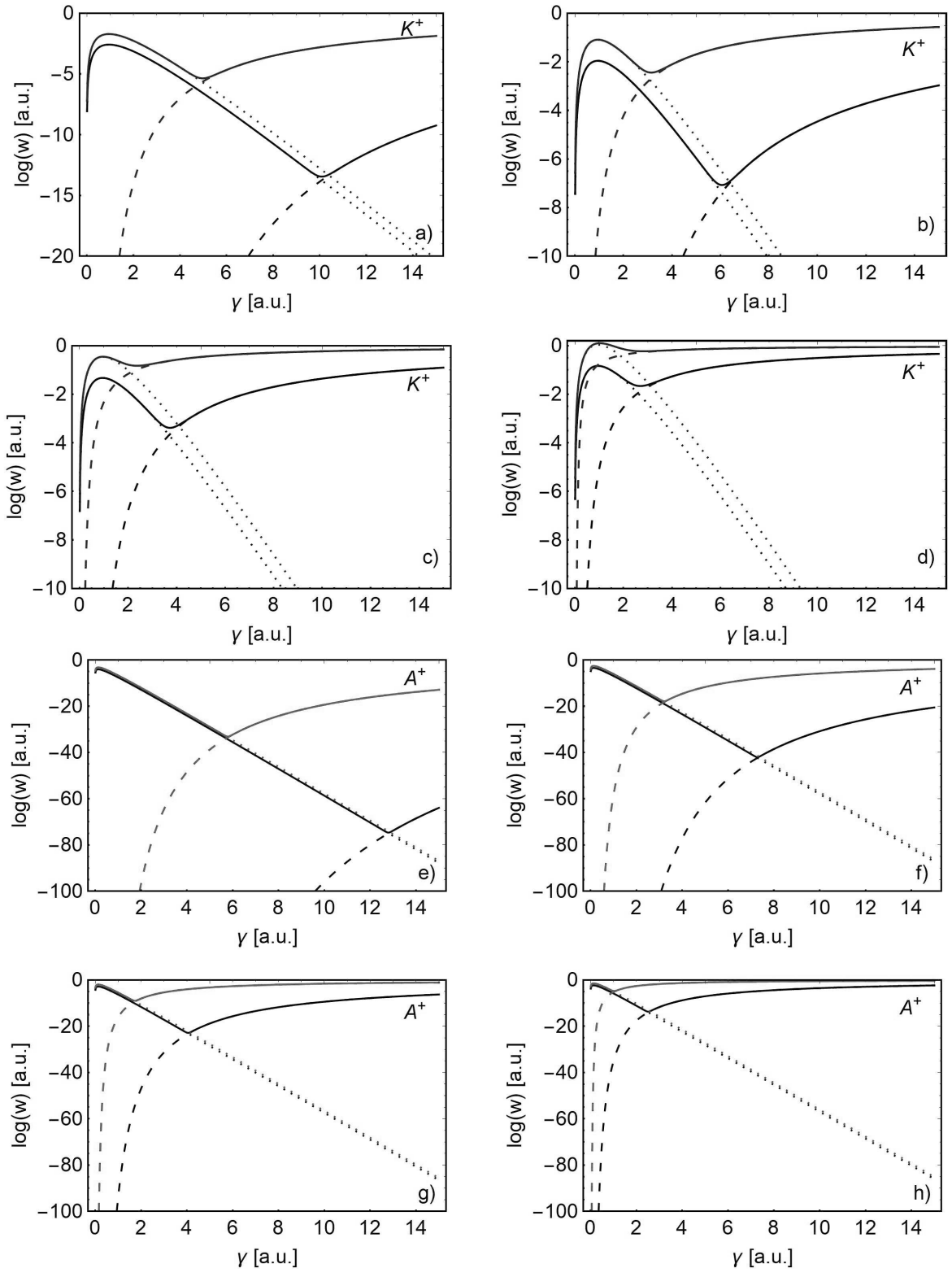

Fig. 2. Ionization transition rates, when the field is spiral amplitude modulated: $w_{tot}^{lin,sp}$ (solid line), $w_{MPI}^{lin,sp}$ (dashed line), $w_{TI}^{lin,sp}$ (dotted line) for potassium represented by blue lines and argon atom by red lines. w_{tot}^{lin} (solid black line), w_{MPI}^{lin} (dashed black line), w_{TI}^{lin} (dotted black line) represent ionization rates for both atoms for the field without spiral amplitude modulated. Both groups of rates are shown as a function of γ parameter at different laser fields intensities: (a) and (e) — at $I = 5.2 \cdot 10^{12}\ \mathrm{W/cm^2}$; ($b$) and ($f$) — at $I = 3.5 \cdot 10^{13}\ \mathrm{W/cm^2}$; ($c$) and ($g$) — at $I = 2.4 \cdot 10^{14}\ \mathrm{W/cm^2}$; ($d$) and ($h$) — at $I = 1.1 \cdot 10^{15}\ \mathrm{W/cm^2}$

be used to investigate the effects of the spiral field amplitude which depends on the spatial variables of ionization parameters.

Photoionization transition rates were calculated using the quantities introduced in the text. Ionization of the valence electron of potassium (K) and argon (Ar) atom by Ti: Sapphire linearly polarized $(0,1)^*$LG laser light at a frequency $\omega = 0.057$ a.u. ($\lambda = 800$nm), with and without the spiral amplitude modulation, was observed. Laser intensities were in the range $I = (10^{12} - 2 \cdot 10^{15})\,\mathrm{W/cm^2}$ which corresponds to the field strength of $F = (0.005 - 0.24)$ a.u., while the ionization potential of valence electron for K-atom $I_p^K = 4.3406\,\mathrm{eV}(0.1595\,\mathrm{a.u.})$ and for Ar-atom $I_p^{Ar} = 15.76\,\mathrm{eV}(0.5791\,\mathrm{a.u.})$.

Note that a radially polarized beam can produce a much smaller focused spot than a common linear polarized beam [46,47] and that the diameter of the laser beam can be dimensions from micrometers $(3-60)$ μm to millimeters $(15-30)$ mm. In our calculations beam diameter is fixed to 3 μm ($5.7 \cdot 10^4$ in atomic unit), $a = 0.57$ ($1.08 \cdot 10^4$ in atomic unit) when r is in μm. The constant $k = \mathrm{ctg}\,\theta$, while θ angle determines spiral geometry and can take value in the range of $[-90°, 90°]$.

TI, MPI and total transition rate were calculated as a function of the γ parameter for various laser intensities (Fig. 2). As can be seen, the total transition rate curve (solid line) has a similar dependence on all four chosen laser intensities. The main characteristic of this curve is that certain values of γ reach a minimum, where the contributions of TI and MPI are equal (hereafter E point). As the laser intensity increases, the position of the minimum shifts to lower γ values. For $I = 5.2 \cdot 10^{12}\,\mathrm{W/cm^2}$ (Fig. 2*a*) the minimum is at $\gamma \approx 10$ for potassium atom and $\gamma \approx 13$ for argon atom (Fig. 2 *e*), while for amplitude modulated field these values are $\gamma \approx 5$ and $\gamma \approx 6$ for potassium and argon atom respectively. In the case of $I = 1.1 \cdot 10^{15}\,\mathrm{W/cm^2}$ (Fig. 2 *d, h*) minimum is at the position of $\gamma \approx 2$ both for the potassium atom and the argon atom for the unmodulated amplitude, while for the spirally modulated amplitude, the gamma value is slightly shifted towards low gamma values.

It should be emphasized that depending on the laser intensities, the absolute values of the minimum of the total transition rate curve also change. At lower laser intensities, the ratio of minimum and maximum value is more than ten orders of magnitude, while for higher fields this ratio is reduced to two orders of magnitude. It can be seen in the figure that TI is dominant for lower values γ, so in this region, the total transition rate coincides with the TI transition curve. On the other hand, the total transition rate coincides with the MPI transition rate in the region where with increasing γ the contribution of MPI becomes significant. The obtained results correspond to the fact that, with increasing gamma, the portion of MPI grows, and vice versa. It is known that, when an atom is exposed to a strong laser field, Stark shift of energy levels becomes significant and the electron gains ponderomotive energy U_p, producing changes in ionization potential I_p, which then becomes dependent on the laser intensity. It is therefore shown how the effective ionization potential affects the ionization rate of the spiral amplitude-modulated laser field.

Summary. We presented a study of the ionization transition rates of potassium and argon atoms in a strong laser field, using the ADK models. We use a linear monochromatic laser source, with a specific $(0,1)^*$LG spiral amplitude modulation and a broad range of intensities. Our calculation covers a wide range of γ values. From this study, we derived the following conclusions: We confirmed that, for the lower values of the Keldysh parameter ($\gamma \leq 1$), tunnelling ionization dominates over multiphoton ionization. It is additionally shown that, with increasing parameter γ, the multiphoton ionization becomes more significant, as for the values of $\gamma \geq 3$, this process presents the main process in the total ionization rate curve, for both atoms. As a consequence of γ dependence, the γ value of the E point moves toward the lower laser intensities. We also found, that the transition rate, at E point, significantly increases for several orders of magnitude with the increase of laser field intensity. We obtained that the influence of the Stark shift and the ponderomotive potential is more noticeable in stronger laser fields, and it is only expressed for the $\gamma \leq 5$. The applied model has limitations for the non-relativistic regime, particularly for laser intensities of $I \leq 10^{18}\,\mathrm{W/cm^2}$. However, it gives satisfying results for lower field intensities.

Acknowledgments. The authors acknowledge funding provided by the University of Kragujevac, Institute for Information Technologies (the contract 451-03-68/2022-14/200378), University of Kragujevac, Faculty of Science (the contract 451-03-68/2022-14/200122) through the grants by the Ministry of Education, Science and Technological Development of the Republic of Serbia.

The full text of this paper is published in the English version of JETP.

REFERENCES

1. M. Hollstein and D. Pfannkuche, Phys. Rev. A **92**, 053421 (2015).

2. K. Hütten, M. Mittermair, S. O. Stock, R. Beerwerth, V. Shirvanyan, J. Riemensberger, A. Duensing, R. Heider, M. S. Wagner, A. Guggenmos, S. Fritzsche, N. M. Kabachnik, R. Kienberger, and B. Bernhardt, Nat. Commun. **9**, 719 (2018).

3. G. Mainfray and G. Manus, Rep. Prog. Phys. **54**, 1333 (1991).

4. A. Sharma, M. N. Slipchenko, M. N. Shneider, X. Wang, K. A. Rahman, and A. Shashurin, Sci. Rep. **8**, 2874 (2018).

5. M. V. Ammosov, P. A. Golovinsky, I. Yu. Kiyan, V. P. Krainov, and V. M. Ristic, J. Opt. Soc. Am. B **9**, 1225 (1992).

6. V. S. Popov, Phys. Usp. **47**, 855 (2004).

7. L. V. Keldysh, Sov. Phys. JETP **20**, 1307 (1965).

8. A. M. Perelomov, V. S. Popov, and M. V. Terent'ev, Sov. Phys. JETP **23**, 924 (1966).

9. M. V. Ammosov, N. B. Delone, and V. P. Krainov, Sov. Phys. JETP **64**, 1191 (1986).

10. H. R. Reiss, Phys. Rev. A **75**, 031404 (2007).

11. X. Hao, Z. Shu, W. Li, S. Hu, and J. Chen, Opt. Express **24**, 25250 (2016).

12. D. T. Lloyd, K. O'Keeffe, and S. M. Hooker, Opt. Express **27**, 6925 (2019).

13. R. Wang, Q. Zhang, D. Li, S. Xu, P. Cao, Y. Zhou, W. Cao, and P. Lu, Opt. Express **27**, 6471 (2019).

14. N. I. Shvetsov-Shilovski, D. Dimitrovski, and L. B. Madsen, Phys. Rev. A **85**, 023428 (2012).

15. H. Wabnitz, A. R. B. de Castro, P. Gürtler, T. Laarmann, W. Laasch, J. Schulz, and T. Möller, Phys. Rev. Lett. **94**, 023001 (2005).

16. A. A. Sorokin, S. V. Bobashev, T. Feigl, K. Tiedtke, H. Wabnitz, and M. Richter, Phys. Rev. Lett. **99**, 213002 (2007).

17. T. Topcu and F. Robicheaux, Phys. Rev. A **86**, 053407 (2012).

18. C. Wang, X. Lai, Z. Hu, Y. Chen, W. Quan, H. Kang, C. Gong, and X. Liu, Phys. Rev. A **90**, 013422 (2014).

19. Y. H. Lai, J. Xu, U. B. Szafruga, B. K. Talbert, X. Gong, K. Zhang, H. Fuest, M. F. Kling, C. I. Blaga, P. Agostini, and L. F. DiMauro, Phys. Rev. A **96**, 063417 (2017).

20. L. Guo, S. L. Hu, M. Q. Liu, Z. Shu, X. W. Liu, J. Li, W. F. Yang, R. H. Lu, S. S. Han, and J. Chen, ArXiv: Atomic Physics (2019).

21. H. Moradi, V. Shahabadi, E. Madadi, E. Karimi, and F. Hajizadeh, Opt. Express **27**, 7266 (2019).

22. S. S. Stafeev, L. O'Faolain, M. I. Shanina (Kotlyar), A. G. Nalimov, and V. V. Kotlyar, Computer Optics **38**, 606 (2014).

23. T. Grosjean, D. Courjon, and C. Bainier, Opt. Lett. **32**, 976 (2007).

24. C. Varin, S. Payeur, V. Marceau, S. Fourmaux, A. April, B.'Schmidt, P-L Fortin, N. Thiré, T. Brabec, F. Légaré, J-C. Kieffer, and M. Piché, Appl. Sci. **3**, 70 (2013).

25. M. Wen, Y. I. Salamin, and C. H. Keitel, Opt. Express **27** 18958 (2019).

26. D. J. Armstrong, M. C. Phillips, and A. V. Smith, Appl. Opt. **42**, 3550 (2003).

27. G. Machavariani, N. Davidson, Y. Lumer, I. Moshe, A. Meir, and S. Jackel, *New Methods of Mode Conversion and Brightness Enhancement in High-Power Lasers, in: Proceedings of the Lasers and Electro-Optics and the International Quantum Electronics Conference*, Munich, 17 – 22 June (2007).

28. J. Ouyang, W. Perrie, O. J. Allegre, T. Heil, Y. Jin, E. Fearon, D. Eckford, S. P. Edwardson, and G. Dearden, Opt. Express **23**, 12562 (2015).

29. G. S. Voronov and N. B. Delone, Sov. Phys. JETP **23**, 54 (1966).

30. M. Uiberacker, Th. Uphues, M. Schultze, A. J. Verhoef, V. Yakovlev, M. F. Kling, J. Rauschenberger, N. M. Kabachnik, H. Schröder, M. Lezius, K. L. Kompa, H.-G. Muller, M. J. J. Vrakking, S. Hendel, U. Kleineberg, U. Heinzmann, M. Drescher, and F. Krausz, Nature **446**, 627 (2007).

31. R. Boge, C. Cirelli, A. S. Landsman, S. Heuser, A. Ludwig, J. Maurer, M. Weger, L. Gallmann, and U. Keller, Phys. Rev. Lett. **111**, 103003 (2013).

32. N. B. Delone, and V. P. Krainov, Physics- Uspekhi **42**, 669 (1999).

33. A. Bunjac, D. B. Popovic, and N. S. Simonovic, ArXiv: Atomic Physics (2019).

34. J. Mitroy, M. S. Safronova, and Ch. W. Clark, J. Phys. B: At., Mol. Opt. Phys. **43**, 20201 (2010).

35. A. Karamatskou, J. Phys. B: At. Mol. Opt. Phys. **50**, 013002 (2017).

36. B. Yang, K. J. Schafer, B. Walker, K. C. Kulander, L. F. DiMauro, and P. Agostini, Acta Phys. Pol. A **86**, 41 (1994).

37. E. A. Volkova, A .M. Popov, and O. V. Tikhonova, J. Exp. Theor. Phys. **113**, 394 (2011).

38. L. Allen, M. W. Beijersbergen, R. J. C. Spreeuw, and J. P. Woerdman, Phys. Rev. A **45**, 8185 (1992).

39. M. Yao and M. J. Padgett, Adv. Opt. Photon. **3**, 161 (2011).

40. M. Uchida and A. Tonomura, Nature **464**, 737 (2010).

41. S. P. Goreslavsky, N. B. Narozhny, and V. P. Yakovlev, J. Opt. Soc. Am. B **46**, 1752 (1989).

42. F. Gori, J. Opt. Soc. Am. A. **18**, 1612 (2001).

43. J. D. Lawrence, *A Catalog of Special Plane Curves*, Dover, New York (1972).

44. D. K. Cheng, *Field and Wave Electromagnetics*, Addison-Wesley Publishing Company (1989).

45. M. J. Padgett and L. Allen. Contemp. Phys. **41**, 275 (2000).

46. R. Dorn, S. Quabis, and G. Leuchs, Phys. Rev. Lett. **91**, 233901 (2003).

47. K. M. Tanvir Ahmmed, C. Grambow, and A. M. Kietzig, Micromachines **5**, 1219 (2014).